

Signal Attenuation Model Free Classification of Diffusion MR Signals of the Breast Tissue using Long Short-Term Memory Networks

Gökhan Ertas

Abstract— Detection and diagnosis of breast cancer from diffusion signals by diffusion-weighted imaging involves in estimation of quantitative metrics by signal attenuation models fitted to the signals. The process suffers from the implementation difficulty of the fitting algorithms and their sensitivity to noise. This study aims development of neural networks to facilitate the classification of the breast tissues from the signals. 37500 diffusion MR signals are synthetically generated for noise-free and noisy conditions by signal-to-noise ratio (SNR) for malignant, benign, and healthy breast tissues. Forty neural networks employing traditional long short-term memory (LSTM) or bidirectional long short-term memory (BiLSTM) blocks up to twenty are trained and tested for the signals using bootstrapping incorporated accuracy analysis. Specificity, sensitivity, and accuracy metrics are computed for the higher performance networks. For noise-free and noisy signals with $\text{SNR} \geq 80$, networks may achieve excellent sensitivities, specificities, and accuracies (100% at all), but LSTM networks require fewer number of memory blocks. For noisy signals having $\text{SNRs} \leq 40$, the networks may deliver high to very high sensitivities (74.8-98.3%), specificities (87.4-99.2%), and accuracies (83.2-98.9%) better for malignant and healthy tissues than benign tissue but BiLSTM ones perform slightly better. LSTM networks eliminate the need for any signal decay model while outputting remarkably good performances in the classification of diffusion signals. BiLSTM networks perform slightly better for very noisy conditions. Prospective studies are needed to justify the potential benefits in a clinical setup.

Index Terms—Breast, classification, diffusion signal, long short-term memory network.

I. INTRODUCTION


DIFFUSION WEIGHTED IMAGING (DWI) makes use of magnetic resonance (MR) principles to deliver diffusion signals from a living tissue captured for a set of increasing diffusion weighting that indirectly reflects the degree of tissue cellularity and the integrity of cell membranes and also the microcirculation of blood in the capillary network by demonstrating the microscopic Brownian motion of water

molecules within the tissue [1]. Due to their high cell density and limited extracellular space, malignant lesions exhibit slowly attenuated diffusion signals for increased diffusion weighting. On the contrary, diffusion signals with fast attenuation due to less restricted diffusion of water molecules are of concern for benign tissues. Besides, healthy tissues may exhibit diffusion signals with similar degrees of attenuation by benign lesions [2]. For human breast tissue, the diffusion-weighted imaging protocol that utilizes diffusion weightings from 0 to 800 s/mm² and the evaluation strategy that practices the apparent diffusion coefficient metric by a mono-exponential signal attenuation model have been promoted as an essential part of multiparametric breast magnetic resonance imaging by the European Society of Breast Radiology (EUSOBI) [3, 4].

The mono-exponential model enables quantitative characterization of the breast tissues from the diffusion signals to distinguish lesions in the detection and diagnosis of cancer. Moreover, it is quite easy to fit the model to diffusion signals to estimate the apparent diffusion coefficient metric. However, the model has a limited capability in expressing the attenuation in the diffusion signal especially for the malignant tissue and therefore advanced models have been under development [5]. The intravoxel incoherent motion (IVIM) model enumerates the attenuation in the diffusion signal using a weighted summation of two exponential functions and is reported to accomplish better sensitivity when compared to the mono-exponential model in distinguishing malignant from benign breast lesions [6, 7]. The IVIM model makes use of three metrics: pure diffusion coefficient, pseudo-diffusion coefficient, and volume fraction for which estimates are obtained by fitting the model to the diffusion signal by using an advanced fitting algorithm. Implementation difficulties of the available algorithms and their sensitivity to noise may lead to metric estimates out of physiologically acceptable ranges making adoption of the model challenging for clinical practice [8-10]. Besides, the diffusion signals may be processed directly without using a fitting algorithm or a signal attenuation model by artificial neural networks.

A diffusion MR signal demonstrates an attenuated amplitude with reference to a monotonically increasing diffusion weighting determined by b -value and can be deliberated as “ b -series” data very similar to time-series data for which the neural networks housing long short-term memory (LSTM) blocks offer better competence in recognizing long-term dependencies and influencing the dependencies into computations as long as they need to be taken into account for classification tasks [11].

GOKHAN ERTAS, is with Department of Biomedical Engineering, Yeditepe University, Istanbul, Turkey, (e-mail: gokhan.ertas@yeditepe.edu.tr).

 <https://orcid.org/0000-0002-3331-9152>

Manuscript received February 7, 2021; accepted May 11, 2021.
DOI: [10.17694/bajece.876291](https://doi.org/10.17694/bajece.876291)

This study aims the development of LSTM neural network models to facilitate the classification of human breast tissue from diffusion MR signals for the detection and diagnosis of breast cancer.

II. MATERIALS AND METHODS

A. Generation of Diffusion Signals for the Breast

The study dataset consists of breast diffusion MR signals generated synthetically by performing the steps illustrated in Fig. 1. The tissue-specific descriptive statistics for the three model parameters of the IVIM model namely the pure diffusion coefficient (D), the pseudo-diffusion coefficient (D^*), and the microvascular volume fraction (f) are entered into excessive analyses incorporating Monte Carlo simulation runs to generate numerous random D , D^* , and f triples for the tissue satisfying the statistics fed. The triples generated are next used to obtain noise-free signals for the tissue by numerically solving the equation $s_b/s_o = (1 - f) \exp(-bD) + f \exp[-b(D^* + D)]$ for a set of b -values [12]. Finally, noise is added to the noise-free signals at the level defined by the signal-to-noise ratio (SNR) to obtain the noisy forms of the signals. In the current work, the descriptive statistics for three breast tissue types are delivered from a recent study stating that on median (lower, upper quartiles), $D = 0.85$ (0.77, 0.98) $\times 10^{-3}$ mm²/s, $D^* = 94.71$ (70.33, 113.23) $\times 10^{-3}$ mm²/s, and $f = 10.34$ (7.68, 11.88) % for the malignant lesion, and $D = 1.35$ (1.26, 1.44) $\times 10^{-3}$ mm²/s, $D^* = 107.49$ (83.20, 131.19) $\times 10^{-3}$ mm²/s, and $f = 6.83$ (4.72, 10.33) % for the benign lesion whereas $D = 1.96$ (1.81, 2.15) $\times 10^{-3}$ mm²/s, $D^* = 124.28$ (113.30, 147.86) $\times 10^{-3}$ mm²/s, and $f = 5.27$ (3.60, 5.87) % for the healthy tissue [13]. For each tissue type, Monte Carlo simulation runs are performed with 2500 repetitions and numerical solutions are computed for ten b -values of 0, 30, 70, 100, 150, 200, 300, 400, 500, 800 s/mm². Random Gaussian noise is deliberated at knowledgeable SNRs of 80, 40, 20, and 10 where SNR is defined as the ratio of the noise-free signal amplitude at $b = 0$ s/mm² to the standard deviation of the noise [9].

B. Design of LSTM Networks for Breast Tissue Classification

Long short-term memory (LSTM) networks are a special type of recurrent neural network that offers better competence in recognizing long-term dependencies and influencing the dependencies into computations to analyzing time-series data for regression and classification tasks. The networks can be implemented using “traditional” LSTM memory blocks that are self-connected subnetworks containing multiple internal cells each having dedicated inputs, outputs, and memory sharable with the other cells in the block [14]. An LSTM memory block can be modified to learn bidirectional long-term dependencies between time steps of time series data and this new block is called bidirectional LSTM (biLSTM) [15].

In the current study, two network models, one housing a traditional LSTM layer and the other consisting of a biLSTM layer are established to classify breast tissues from b -series data from the diffusion MR signals generated. The models have the same layer structure as presented in Fig. 2. The first layer is the sequence input layer that accepts the “ b -series data” of the diffusion signal of breast tissue to the network. The second

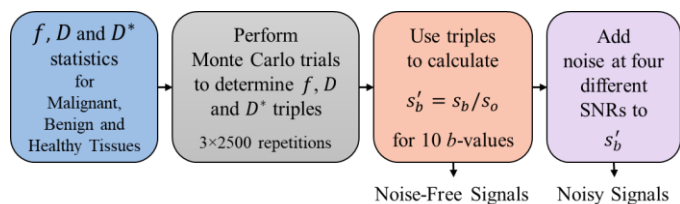


Fig. 1: The framework of synthetic diffusion MR signal generation.

layer is the LSTM layer for the first model and the biLSTM layer for the second model that learns long-term dependencies between b -values and diffusion MR signal attenuation. The third layer is the fully connected layer that multiplies the output of the LSTM/biLSTM layer by a weight matrix and then adds a bias vector to provide three outputs dedicated to the malignant, benign and healthy breast tissue types. The next layer is the Softmax layer that applies the Softmax function to the outputs of the fully connected layer. The outputs of this layer are evaluated and classification is made concerning the output that provides the largest value. However, during network training, a classification layer is appended to the network to compute loss for the multi-class classification on the outputs of the Softmax layer. During the implementation of the models, neural networks with varying numbers of memory blocks up to twenty are considered for each model.

C. Training and Testing of Neural Networks

The neural networks implemented are trained using the same training parameters: 300 epochs, a batch size of 125, an initial learning rate of 5×10^{-4} , a gradient threshold of 1, and an adaptive moment estimation optimizer with the cross-entropy loss [16]. Bootstrapping incorporated accuracy analyses are performed to train and then to test the networks [17]. For this purpose, the diffusion MR signals generated are assigned as the original dataset, and twenty bootstrapped datasets, each consisting of random resamples from the original dataset with the same number of signals for each tissue type in the original dataset, are formed.

A network is first trained using the original dataset and on the outputs of the network, an “apparent” accuracy, Acc^{app} is computed. The network is next trained with the bootstrapped datasets and the outputs of the network for the datasets are processed to compute “bootstrap-sample” accuracies, Acc^{bs} . Besides, after completion of a training, the network is tested using the original dataset and the outputs are explored to compute “original-sample” accuracies, Acc^{os} . The differences between Acc^{bs} and Acc^{os} pairs are computed and then averaged to calculate an overall optimism value. By subtracting the overall optimism from Acc^{app} , the “corrected” accuracy, Acc^c is determined for each network. The network having an Acc^{os} closest to Acc^c is deemed the best network.

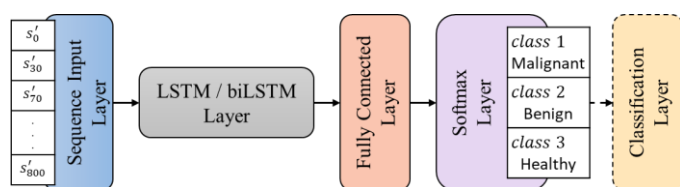


Fig. 2: The LSTM/biLSTM network model to classify breast tissues from the diffusion MR signals of the tissues.

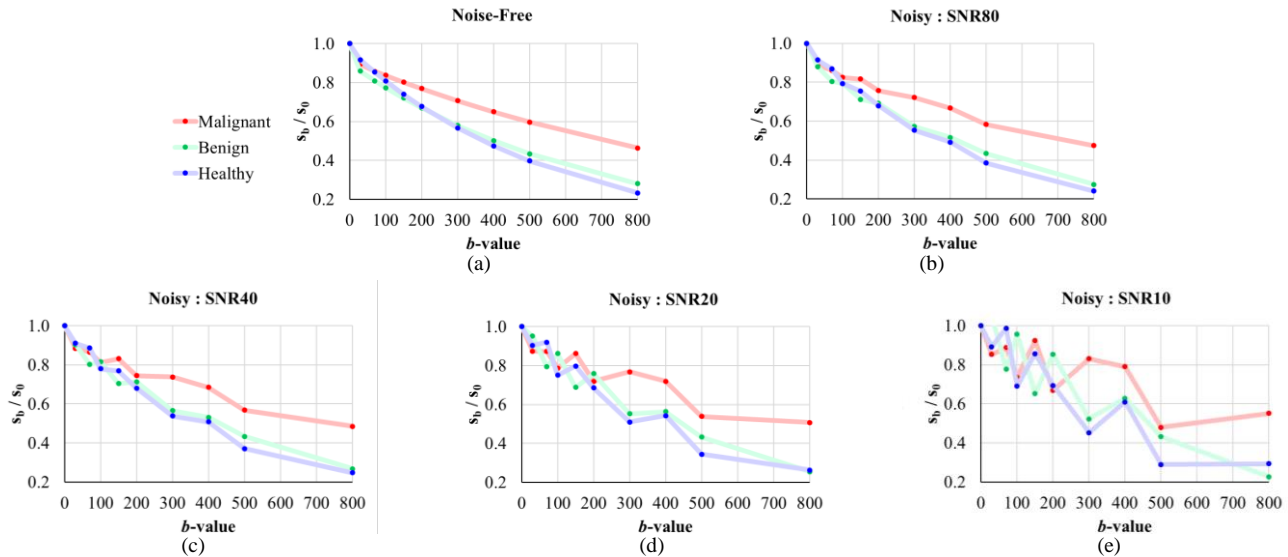


Fig.3: Diffusion MR signals generated using IVIM parameters for the malignant ($D = 0.84 \times 10^{-3} \text{ mm}^2/\text{s}$, $D^* = 84.42 \times 10^{-3} \text{ mm}^2/\text{s}$, and $f = 8.99\%$), benign ($D = 1.45 \times 10^{-3} \text{ mm}^2/\text{s}$, $D^* = 133.08 \times 10^{-3} \text{ mm}^2/\text{s}$, and $f = 10.55\%$), and healthy tissue ($D = 1.77 \times 10^{-3} \text{ mm}^2/\text{s}$, $D^* = 110.17 \times 10^{-3} \text{ mm}^2/\text{s}$ and $f = 3.41\%$) considering b -values of 0, 30, 70, 100, 150, 200, 300, 400, 500, 800 s/mm^2 . (a) Noise-free signals, and (b-e) noisy versions of the signals produced for the noise levels expressed by the SNRs of 80, 40, 20, and 10.

D. Assessment of the Neural Network Performance

The performance of the best neural network is assessed using the sensitivity (Se), specificity (Sp), and accuracy (Acc) metrics estimated from the outputs of the network for the original dataset using

$$Se_i = \frac{TP_i}{TP_i + FN_i} \quad (1a)$$

$$Sp_i = \frac{TN_i}{TN_i + FP_i} \quad (1b)$$

$$Acc_i = \frac{TP_i + TN_i}{TP_i + FN_i + TN_i + FP_i} \quad (1c)$$

Here: TP – is true-positive,
 FP – is false-positive,
 TN – is true-negative,
 FN – is false-negative classifications by the neural network for the i -th tissue class.

Overall values for the metrics are calculated by summing the performance for a class and dividing the result by three. The metrics are considered very high, high, moderate, low, and very low if their values were 95%-100%, 85%-94.9%, 75%-84.9%, 65%-74.9%, and 0%-64.9%, respectively. The neural networks are numerically implemented and analyzed using our in-house computer software tools developed using MATLAB (v8.2; Natick, MA) on a desktop PC (Intel i7-1065G7 3.90GHz processor, 16GB memory, and 64-bit operating system).

III. RESULTS

A total of 37500 diffusion MR signals (7500 noise-free and 30000 noisy) are synthetically generated for malignant, benign, and healthy tissues of the human breast. Fig.3 illustrates sample signals for each breast tissue type for noise-free and noisy conditions expressed using the SNR. Signal attenuation is characterized very well using the IVIM model for the noise-free

signals but the model has difficulty describing the attenuation for the noisy signals. Meanwhile, available fitting algorithms probably output misleading estimates for the D , D^* and f metrics especially for lower SNRs resulting in incorrect classifications.

A total of forty neural networks are developed to perform tissue classification from diffusion MR signals. Twenty networks are relying on an LSTM model, while the remaining networks are based on a BiLSTM model. The networks are implemented with the same layer structure but with different numbers of memory blocks up to twenty in the LSTM/biLSTM layer. By bootstrapping incorporated accuracy analysis, twenty-one training and testing tasks are performed for each network and a total of 840 training and testing tasks are handled at all. Plots for the “corrected” accuracies for the networks for the noise-free and the noisy conditions are seen in Fig. 4. The LSTM and BiLSTM network models reveal very similar moderate to very high accuracies that improve when SNR increases. The accuracy also improves when a larger number of memory blocks is utilized in the models for a specific SNR. The accuracy reaches its maximum value of 100% for the noise-free signals and the noisy signals with an SNR of 80 for both models. Lower accuracies are of concern for the models for the noisy signals with $\text{SNR} \leq 40$. When SNR is reduced to 40, the LSTM and BiLSTM models provide high to very high accuracies (range: 88.1-98.2% and 88.6-98.9%, mean: 97.1% and 97.2%). For SNR of 20, high accuracies are delivered by the models (range: 86.1-92.4% and 86.2-92.6%, mean: 91.7% and 91.5%). When SNR is further reduced to 10, the models offer moderate to high accuracies (range: 79.3-83.4% and 80.5-83.2%, mean: 82.9% and 82.8%). Higher accuracies are achieved for the models when they are implemented using three or more memory blocks in their LSTM/biLSTM layer. Change in the number of memory blocks results in fewer accuracy variations for the LSTM model while that may cause large fluctuations in the accuracy for the biLSTM model.

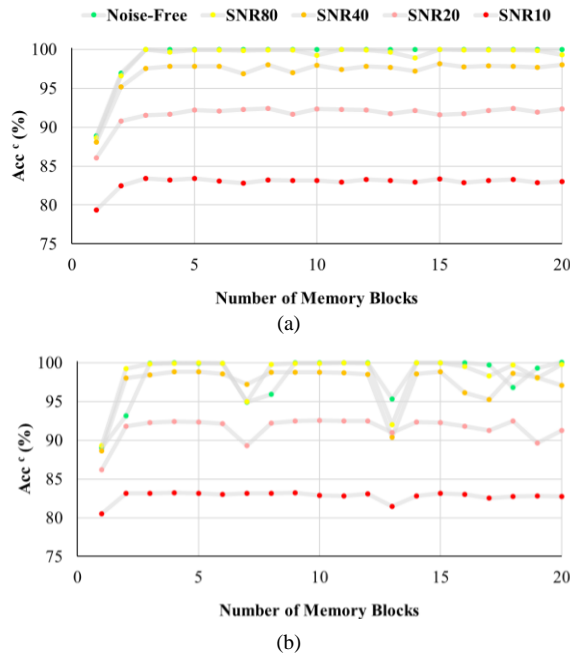


Fig.4: “Corrected” accuracy for the number of memory blocks for the (a) LSTM and (b) biLSTM network models.

The attributes and the classification performances of the best networks by the network model and the noise level are listed in Table I. Corresponding bar graphs for the accuracy and the number of memory blocks of the networks are seen Fig. 5. Use of the LSTM model leads to networks with three memory blocks, while the biLSTM model induces networks with nine and fourteen memory blocks to classify the noise-free and the noisy signals with SNR of 80 of the malignant, benign and healthy breast tissues. The overall performances of the networks are excellent at all ($Se= 100.0\%$, $Sp= 100.0\%$, and $Acc= 100.0\%$). For SNR of 40, the models both convey networks with fifteen memory blocks that perform very good, however, a reasonably better overall performance is offered by the BiLSTM model based network ($Se= 98.3\%$, $Sp= 99.2\%$, and $Acc= 98.9\%$) compared to the LSTM model based network ($Se= 97.2\%$, $Sp= 98.6\%$, and $Acc= 98.2\%$). For SNR of 20, the biLSTM model induces a network with ten memory blocks ($Se= 88.9\%$, $Sp= 94.5\%$, and $Acc= 92.7\%$) that performs

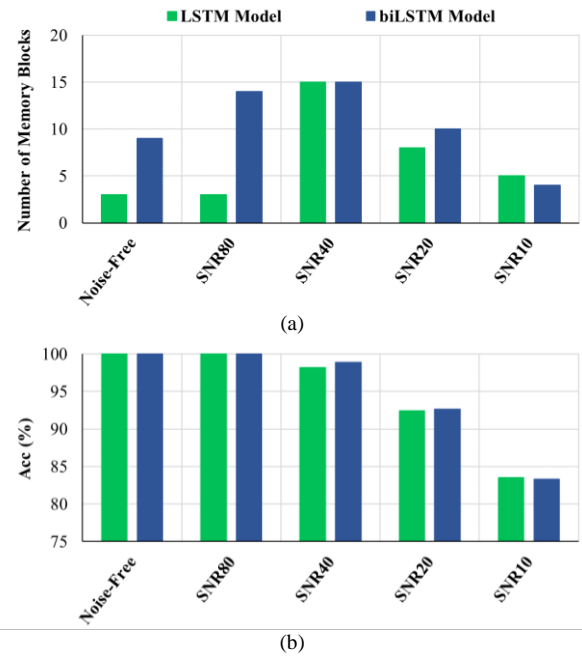


Fig.5: Best networks by the LSTM and BiLSTM network models. (a) Number of memory blocks and (b) overall classification accuracy.

slightly better than the network with eight memory blocks by the LSTM model ($Se= 88.6.2\%$, $Sp= 94.3\%$, and $Acc= 92.4\%$). For SNR of 10, the biLSTM model introduces a network with four memory blocks that performs good ($Se= 74.8\%$, $Sp= 87.4\%$, and $Acc= 83.2\%$), however, a slightly better performance is achieved by the LSTM model by a network with five memory blocks ($Se= 75.1\%$, $Sp= 87.6\%$, and $Acc= 83.4\%$).

Regardless of the model that it relies on, a network may achieve excellent sensitivities, specificities, and accuracies in the classification of the malignant, benign and healthy breast tissues for SNRs ≥ 80 and noise-free cases. On the other hand, for SNRs ≤ 40 , an LSTM network delivers very high to high sensitivities, specificities, and accuracies better for malignant and healthy tissues than benign tissue; however, a biLSTM network performs slightly better than the LSTM one.

TABLE I
THE ATTRIBUTES AND PERFORMANCES OF THE BEST NEURAL NETWORKS

		Noise-Free		Noisy : SNR80		Noisy : SNR40		Noisy : SNR20		Noisy : SNR10	
		LSTM	biLSTM	LSTM	biLSTM	LSTM	biLSTM	LSTM	biLSTM	LSTM	biLSTM
Number of Memory Blocks		3	9	3	14	15	15	8	10	5	4
Acc (%)	Overall	100	100	100	100	98.2	98.9	92.4	92.7	83.4	83.2
	Malignant	100	100	100	100	98.5	99.1	93.9	94.1	86.8	86.7
	Benign	100	100	100	100	97.3	98.3	88.6	89.0	75.3	75.0
	Healthy	100	100	100	100	98.8	99.1	94.7	94.9	88.1	87.9
Se (%)	Overall	100	100	100	100	97.2	98.3	88.6	88.9	75.1	74.8
	Malignant	100	100	100	100	97.2	98.5	91.5	90.3	78.4	75.8
	Benign	100	100	100	100	96.3	97.9	83.4	84.6	63.5	63.9
	Healthy	100	100	100	100	98.2	98.4	90.9	91.9	83.4	84.6
Sp (%)	Overall	100	100	100	100	98.6	99.2	94.3	94.5	87.6	87.4
	Malignant	100	100	100	100	99.1	99.5	95.2	96.0	91.1	92.1
	Benign	100	100	100	100	97.7	98.5	91.2	91.1	81.2	80.5
	Healthy	100	100	100	100	99.0	99.5	96.5	96.3	90.4	89.5

IV. DISCUSSIONS

Long short-term memory (LSTM) networks offer competence in recognizing long-term dependencies and influencing the dependencies into computations in classifying time-series data and their use has been gaining increased interest in medicine predominantly for detection of medical events from electronic health records, classification of diseases from physiological signals and segmentation of lesions from medical images [18-22]. Besides, an LSTM network has been proposed to distinguish malignant and benign breast tissues using the features extracted by a fine-tuned VGGNet from dynamic contrast-enhanced MR signals pondered as “contrast-enhanced time-series data” [23]. The current study inspires LSTM networks for classifying human breast tissues from diffusion MR signals that can be deliberated as “*b*-series data”. Many LSTM networks relying on the traditional LSTM model and the bidirectional LSTM (biLSTM) model are developed to classify the malignant, benign, and healthy tissues from noise-free and noisy signals expressed with signal-to-noise ratio (SNR). Results show that regardless of the model it relies on, an LSTM network may achieve excellent sensitivities, specificities, and accuracies in classifying the tissues from noise-free signals and also from noisy signals with SNRs ≥ 80 . These performances are supplied by fewer number of memory blocks when the network is implemented using the traditional LSTM model. For noisy signals having SNRs ≤ 40 , a network may deliver high to very high sensitivities, specificities, and accuracies better for the malignant and healthy tissues than the benign tissue regardless of the model it relies on. However, a biLSTM model based network would perform slightly better than a traditional LSTM model based one by supplying an effectively increased amount of data to the network.

There are some limitations of the current study. The diffusion MR signals for the malignant, benign and healthy breast tissues are generated by processing the descriptive statistics of the IVIM model parameters reported from a single-center study [13] and therefore may not be generalized well. Noisy versions of the signals are produced considering Gaussian noise and acknowledgeable range and definition for SNR that might imitate the noise in practice in a limited way. The networks developed house either LSTMs or biLSTMs populated in a single layer and the adoption of additional layers may improve the performances of the networks. Moreover, the networks are trained using a “cross-entropy” loss and better trainings can be accomplished using more sophisticated measures such as “AUC loss” [24] that may further improve the classification performances. The networks are trained using bootstrap incorporated accuracy analysis and the use of alternative methods such as k-fold cross validation may lead to different performances by the networks [25].

In conclusion, LSTM networks eliminate the need for any signal decay model while outputting remarkably good performances in the classification of diffusion MR signals of the human breast tissue. BiLSTM networks perform slightly better for very noisy conditions. Prospective studies are needed to justify the potential benefits in a clinical setup.

REFERENCES

- [1] G.S. Chilla, C.H. Tan, C. Xu, C.L. Poh. “Diffusion weighted magnetic resonance imaging and its recent trend-a survey.” *Quantitative imaging in medicine and surgery*, vol. 5, no. 3, 2015, pp. 407-422.
- [2] L. Tang, and X.J. Zhou. “Diffusion MRI of cancer: From low to high b-values.” *J. Magn. Reson. Imaging*, vol. 49, 2019, pp. 23-40.
- [3] R. Woodhams, S. Ramadan, P. Stanwell, S. Sakamoto, H. Hata, M. Ozaki, S. Kan, Y. Inoue. “Diffusion-weighted imaging of the breast: Principles and clinical applications.” *RadioGraphics*, vol. 31, 2011, pp. 1059-1084.
- [4] P. Baltzer, R.M. Mann, M. Iima, E.E. Sigmund, P. Clauser, F.J. Gilbert, L. Martincich, S.C. Partridge, A. Patterson, K. Pinker, F. Thibault et al. “Diffusion-weighted imaging of the breast-a consensus and mission statement from the EUSOBI International Breast Diffusion-Weighted Imaging working group.” *Eur Radiol.*, vol. 30, no. 3, 2020, pp. 1436-1450.
- [5] D. Le Bihan, and M. Iima. “Diffusion magnetic resonance imaging: What water tells us about biological tissues.” *PLoS Biol.*, vol. 13, 2015, e1002203.
- [6] M. Zhao, K. Fu, L. Zhang, W. Guo, Q. Wu, X. Bai, Z. Li, Q. Guo, J. Tian. “Intravoxel incoherent motion magnetic resonance imaging for breast cancer: A comparison with benign lesions and evaluation of heterogeneity in different tumor regions with prognostic factors and molecular classification”. *Oncology Letters*, vol. 16, 2018, pp. 5100-5112.
- [7] Y. Kim, K. Ko, D. Kim, C. Min, S.G. Kim, J. Joo, and B. Park. “Intravoxel incoherent motion diffusion-weighted MR imaging of breast cancer: association with histopathological features and subtypes.” *Br. J. Radiol.*, vol. 89, no. 1063, 2016, pp. 20160140.
- [8] N.R. Doudou, Y. Liu, S. Kampo, K. Zhang, Y. Dai, S. Wang. “Optimization of intravoxel incoherent motion (IVIM): variability of parameters measurements using a reduced distribution of b values for breast tumors analysis.” *MAGMA*, vol. 33, 2020, pp. 273-281.
- [9] G.Y. Cho, L. Moy, J.L. Zhang, S. Baete, R. Lattanzi, M. Moccaldi, J.S. Babb, S. Kim, D.K. Sodickson, E.E. Sigmund. “Comparison of fitting methods and b-value sampling strategies for intravoxel incoherent motion in breast cancer.” *Magn. Reson. Med.*, vol. 74, no. 4, 2015, pp. 1077-1085.
- [10] G. Ertas. “Fitting intravoxel incoherent motion model to diffusion MR signals of the human breast tissue using particle swarm optimization.” *An International Journal of Optimization and Control: Theories & Applications (IJOCTA)*, vol. 9, no.2, 2019, pp. 105-112.
- [11] G. Van Houdt, C. Mosquera, and G. Nápoles. “A review on the long short-term memory model.” *Artif. Intell. Rev.*, vol. 53, 2020, pp. 5929-5955.
- [12] D. Le Bihan, E. Breton, D. Lallemand, P. Grenier, E. Cabanis, and M. Laval-Jeantet. “MR imaging of intravoxel incoherent motions: application to diffusion and perfusion in neurologic disorders.” *Radiology*, vol. 161, no. 2, 1986, pp. 401-417.
- [13] C. Liu, C. Liang, Z. Liu, S. Zhang, B. Huang. “Intravoxel incoherent motion (IVIM) in evaluation of breast lesions: Comparison with conventional DWI.” *European Journal of Radiology*, vol. 82, no. 12, 2013, pp. e782-e789,
- [14] S. Hochreiter and S. Jürgen. “Long short-term memory.” *Neural computation*, vol. 9, no. 8, 1997, pp. 1735-1780.
- [15] M. Schuster and P.K. Kuldip. “Bidirectional Recurrent Neural Networks.” *IEEE Trans. Signal Processing*, vol. 45, no. 11, 1997, pp. 2673-2681.
- [16] D. P. Kingma, and J. Ba. “Adam: A method for stochastic optimization.” *arXiv preprint arXiv:1412.6980*, 2014.
- [17] F.E. Harrell, K.L. Lee, D.B. Mark. “Multivariable prognostic models: issues in developing models, evaluating assumptions and adequacy, and measuring and reducing errors.” *Stat Med.*, vol. 15, no. 4, 1996, pp. 361-387.
- [18] J. Chu, W. Dong, K. He, H. Duan, Z. Huang. “Using neural attention networks to detect adverse medical events from electronic health records.” *Journal of Biomedical Informatics*, vol. 87, 2018, pp. 118-130.
- [19] B. Rim, N.J. Sung, S. Min, M. Hong. “Deep learning in physiological signal data: A survey.” *Sensors (Basel)*, vol. 20, no. 4, 2020, pp. 969.
- [20] P. Nagabushanam, S. Thomas George, S. Radha. “EEG signal classification using LSTM and improved neural network algorithms.” *Soft Computing*, vol. 24, 2020, pp. 9981-10003.
- [21] S. Saadatnejad, M. Oveisi, M. Hashemi. “LSTM-Based ECG classification for continuous monitoring on personal wearable devices. *IEEE J. Biomed. Health Inform.*, vol. 24, no. 2, 2020, pp. 515-523.
- [22] M.H. Hesamian, W. Jia, X. He, P. Kennedy. “Deep learning techniques for medical image segmentation: Achievements and challenges.” *J. Digit. Imaging.*, vol. 32, no. 4, 2019, pp. 582-596.

- [23] N. Antropova, B. Huynh, H. Li, M.L. Giger. "Breast lesion classification based on dynamic contrast-enhanced magnetic resonance images sequences with long short-term memory networks." *J. Med. Imaging (Bellingham)*, vol. 6, 2018, 011002.
- [24] S. Gultekin, A. Saha, A. Ratnaparkhi, J. Paisley. "MBA: Mini-Batch AUC Optimization." *IEEE Transactions on Neural Networks and Learning Systems*, vol. 31, no. 12, 2020, pp. 5561-5574.
- [25] J.H Kim. "Estimating classification error rate: Repeated cross-validation, repeated hold-out and bootstrap." *Computational Statistics & Data Analysis*, vol. 53, no. 11, 2009, pp. 3735-3745.

BIOGRAPHIES



GOKHAN ERTAS Istanbul, in 1976, received his B.S. degree from Erciyes University in Electronics Engineering in 1998 and his M.S. and Ph.D. degrees from Bogazici University in Biomedical Engineering in 2001 and 2007, respectively. He led efforts in developing computational methods to comparing breast MR images at the

Institute of Cancer Research and the Royal Marsden Hospital, UK. He is currently the vice-chairman of the Biomedical Engineering Department at Yeditepe University. His interests include machine learning methods for better characterization of breast tissues to improve the detection and diagnosis of breast cancer using MR imaging.